CMLS, Cell. mol. life sci. 53 (1997) 871–887
1420-682X/97/120871-17 $ 1.50 + 0.20/0

CMLS Cellular and Molecular Life Sciences

The molecular basis of amyloidosis

L. C. Serpell[a], M. Sunde[a,b,*] and C. C. F. Blake[a,b]

[a]Laboratory of Molecular Biophysics, University of Oxford, The Rex Richards Building, South Parks Road, Oxford, OX1 3QU (UK)
[b]Oxford Centre for Molecular Sciences, University of Oxford, New Chemistry Laboratory, South Parks Road, Oxford, OX1 3QT (UK)

Abstract. Amyloidoses are diseases, including some currently prominent such as Alzheimer's disease, bovine spongiform encephalophaty (BSE) and Type II diabetes, in which soluble proteins are deposited in a specific, highly stable, fibrillar form. The amyloid fibrils are made up of protofilaments whose molecular structure is composed of pairs of β-sheets in a helical form that allows them to be continuously hydrogen-bonded along the length of the fibril. The observation that similar fibrils are generated from different proteins indicates that fibril formation is accompanied by structural conversion. The transmissible spongiform encephalopathies, such as BSE and kuru, involve an infectious agent identified with the prion protein. The properties of the agent are more consistent with prion amyloid than the protein itself, suggesting infectivity in these diseases is equivalent to the 'seeding' of amyloid fibrils at a new site.

Key words. Amyloid; amyloidosis; fibrils; protofilaments; Alzheimer's disease; spongiform encephalopathies; fibre diffraction; cross-β conformation.

Introduction

Amyloidosis is a disorder of protein metabolism, acquired or inherited, in which normally soluble proteins are deposited in a particular fibrillar form in the extracellular space of organs and tissues. Amyloid deposits usually persist and accumulate, leading progressively to death through organ failure. Organ transplant may ameliorate some amyloidotic conditions, but for most there is at present no effective treatment. Amongst the known amyloid diseases are some of the most currently prominent of our time. They include Alzheimer's disease, now the fourth most common cause of death in the Western world, the transmissible spongiform encephalopathies, including bovine spongiform encephalopathy (BSE or 'mad cow disease') and its human forms Creutzfeldt-Jakob disease (CJD) and kuru, Type II or non-insulin-dependent diabetes and a number of polyneuropathies and other diseases. Fifteen different proteins are known to form amyloid in vivo, either as a result of genetic mutation, incorrect processing or abnormal accumulation of wild-type proteins. Each amyloidogenic protein is associated with a specific amyloidosis.

In spite of the involvement of quite distinct proteins, there is a body of evidence that indicates that the different amyloid fibrils that are composed of these proteins have the same basic molecular form. All amyloid fibrils seem to exhibit the following molecular properties, which are now considered to be diagnostic for amyloid:

1) Appearance in the electron microscope. Amyloid fibrils examined under the electron microscope show uniform fibrils about 100 Å in diameter. The fibrils are straight and unbranched, and show a smooth surface lacking any very obvious surface features (fig. 1).

* Corresponding author. Pesent address: Oxford Centre for Molecular Sciences, University of Oxford, New Chemistry Laboratory, South Parks Road, Oxford, OX1 3QT (UK), Fax: +44 1865 275921, e-mail: margie@bioch.ox.ac.uk

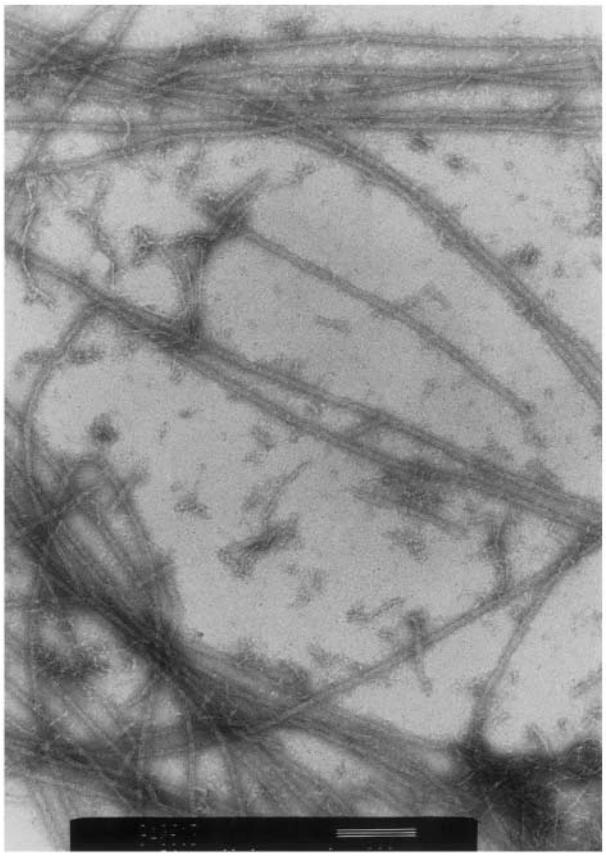

Figure 1. Electron micrograph of transthyretin Val30Met fibrils. Electron micrograph of Val30Met transthyretin amyloid fibrils from the vitreous humour. The fibrils were negatively stained with uranyl acetate. The scale bar represents 200 nm.

2) Tinctorial properties. All amyloid fibrils can be stained with the diazo dye Congo Red, and exhibit an apple-green birefringence which is the most widely used diagnostic test for amyloid. It is likely that the Congo Red molecule is bound and ordered in a specific way by the amyloid fibrils, but the interaction remains to be characterized.

3) X-ray diffraction pattern. Amyloid fibrils give rise to characteristic X-ray fibre diffraction patterns dominated by relatively sharp and intense 4.7-Å meridional and weaker and more diffuse 10-Å equatorial reflections (fig. 2). This pattern is indicative of a particular type of β-sheet structure, known as the cross-β structure, in which β-sheets are arranged parallel to the axis of the fibres with their constituent β-strands *perpendicular* to the fibre axis. This is different from the bulk of the insect β-silks in which the strands of the β-sheets are *parallel* to the fibre axis.

These same characteristics seem to occur in amyloid fibrils from different amyloid diseases and from different precursor proteins. They are also observed in fibrillar material that results from the in vitro denaturation of certain proteins and also from the polymerization of many oligopeptides. The production of apparently similar protein fibrils from a variety of different proteins in disease, and from spontaneous processes in the laboratory, involving polypeptide chains of quite different lengths and native structures and amino acid sequences is an intriguing phenomenon. On the basis of these observations, amyloidosis can be seen to represent a specific and unusual process in protein science, with much remaining to be discovered. At the same time, understanding the process of amyloid formation may indicate targets for the development of drugs to treat the amyloid diseases, which are now so urgently required.

The structural hierarchy: fibrils, protofilaments and sub-protofilaments

Following the pioneering electron microscope studies of amyloid by Cohen and Calkins [1], which demonstrated its essential fibrillar nature, the numerous subsequent studies carried out in different laboratories have tended largely to confirm the conclusions of the earliest investigators. The principal characteristics of the amyloid fibril observable by electron microscopy were comprehensively described by Shirahama and Cohen [2]. Working with ex vivo fibrils isolated from patients with secondary amyloidosis (composed of fragments of the SAA protein or the immunoglobulin light chain), they described the fibrils as being 75–80 Å in diameter, and being composed of five (or less likely six) protofilaments, each about 25–35 Å wide, arranged parallel to one another, longitudinal or slightly oblique to the long axis of the fibril. In turn, the protofilaments appear to be composed of two or three subunit strands 10–15 Å wide (termed sub-protofilaments), helically arranged with a 35–50 Å repeat. In a review of the electron microscopy of amyloid over the next 15 years, Cohen and his colleagues [3] were able to show that this model had been largely confirmed.

Although not contradicting the early ultrastructural model of amyloid, more recent studies have extended the model and the concept of the amyloid fibril in a useful way. The earlier studies had tended to view amyloid as if it were a single, specific type of material with a single set of structural characteristics. Different appearances of fibrils in the electron microscope fields were ascribed to different angles of viewing or different depths or degrees of staining. Although these aspects are clearly important, it is evident now that while different amyloids belong to the same class of substance, with a similar or identical core structure, there are some significant, albeit possibly superficial, differences between amyloids composed of different proteins.

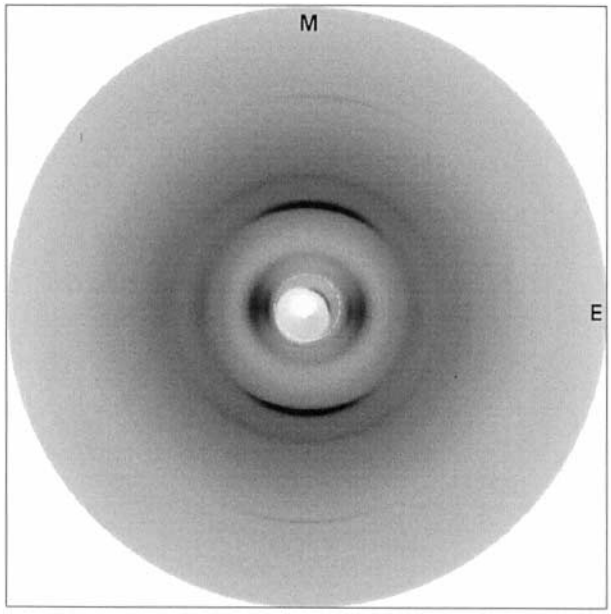

Figure 2. X-ray fibre diffraction pattern from synthetic amyloid fibrils. The fibril sample is composed of a ten-residue peptide with the sequence of the A-strand of transthyretin, which forms amyloid fibrils spontaneously when dissolved in water. The fibrils were aligned in a magnetic field to improve alignment. The diffraction pattern shows the dominant reflections at 4.7–4.8 Å on the meridian (M) and approximately 10 Å on the equator (E).

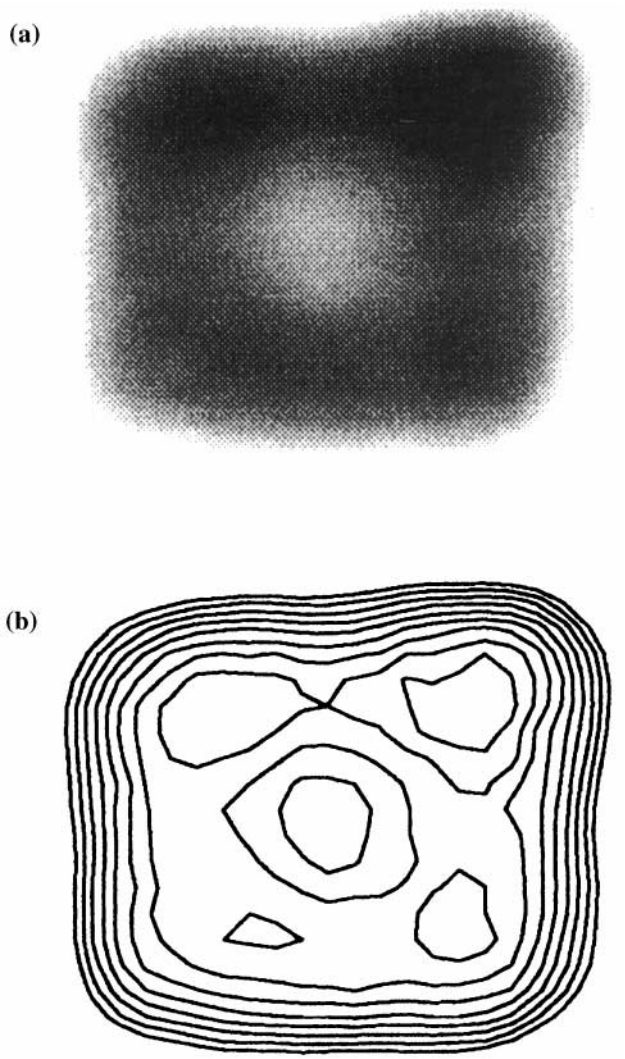

Figure 3. Cross-section of Val30Met transthyretin amyloid fibrils. (*a*) Averaged image of a Val30Met transthyretin fibril (as in fig. 1) from the vitreous humour obtained by summation of the individual densities after translational and rotational alignment by cross-correlation. (*b*) Averaged image as in (*a*), but represented as a density contour plot [8].

The most thorough electron microscope analysis made so far is that reported for the ex vivo amyloid fibrils composed of Val30Met transthyretin (TTR), associated with the most common type of familial amyloidotic polyneuropathy (FAP). These fibrils were extracted from the vitreous humour of the eye. These fibrils have been subjected to modern image reconstruction techniques in both longitudinal and transverse sections. This study demonstrates clearly the lack of any regular pronounced surface features repeating along the fibril, but shows that in transverse sections the observed 120-Å-diameter fibrils are composed of four 60-Å-diameter protofilaments in a square-section array (fig. 3). The protofilaments appear to run more or less parallel to the axis of the fibril, suggesting unexpectedly that there is little or no helical character at this level of the structure. Other electron microscope studies, although less rigorous than that on the Val30Met FAP fibrils, show fibrils composed of different numbers of differently sized protofilaments as listed in table 1.

From these and earlier electron microscope studies, it is now clear that amyloid fibrils derived from different polypeptide precursors may be composed of different numbers and/or arrangements of protofilaments [2, 7, 8]. There are also indications that the diameters of the protofilaments are somewhat variable. These two types of variation can combine to produce variability in the transverse dimensions of amyloid fibrils. Not enough is known at present to be sure of the real significance of these differences in the substructure of different amyloid fibrils. Although the variations may reflect fundamental differences in the molecular properties, it is also possible to accommodate this degree of variability within a common molecular structure for amyloid (see section entitled 'A common core structure for amyloid fibrils'), in which case these differences may be superficial. One experimental demonstration that different fibril substructure may reflect slight or superficial changes at the

Table 1. Substructure of amyloid fibrils.

Amyloid protein	Fibril dimensions	Substructure	Reference
Serum amyloid A or Ig light chain	75–80 Å diameter	five 25–35 Å protofilaments in pentagonal array	[2]
Transthyretin (FAP)	130 Å diameter	four 50–60 Å protofilaments in square section array	[8]
Ab peptide	90 Å diameter	five or six 25–30 Å protofilaments in pentagonal or hexagonal array	[4]
Calcitonin	50–60 Å diameter	?	[5]
Prion	60–200 Å ribbons	flat assembly of ? protofilaments	[6]

molecular level is the marked variation in morphology observed with synthetic Alzheimer's amyloid at different pH values [7].

The development of the cross-β model for amyloid structure

The α-(helix) and β-(sheet) structures of polypeptide chains were initially differentiated by their characteristic X-ray fibre diffraction patterns [9]. The particular conformations that gave rise to these patterns were derived much later from model-building studies that sought to exploit the ability of the peptide group to form multiple interpeptide hydrogen bonds. In the β-structure as described by Pauling and Corey [10], the polypeptide chain is in an extended conformation with alternate peptide groups rotated by 180° (as shown in fig. 4). In this conformation, each CO and NH group in any one β-strand can make hydrogen bonds between the NH or CO groups, respectively, on adjacent β-strands lying parallel or antiparallel to it. Since these neighbouring strands can in turn make hydrogen bonds to further similarly organized β-strands, the β-structure has an inherent propensity to form structures in which an indefinite number of β-strands may be hydrogen-bonded together into very stable, extended, sheet-like assemblies.

The standard length of hydrogen bonds between CO and NH groups of 2.9 Å of adjacent β-strands fixes the separation of adjacent β-strands in the β-sheet rather precisely at about 4.7 Å. Therefore, when the β-strands are perpendicular to the fibre axis, as occurs in the cross-β structure, the regular 4.7-Å separation of successive β-strands along the axis of the fibril will give rise to an intense 4.7-Å reflection that dominates the meridional X-ray diffraction pattern. The presence of two or more β-sheets arranged parallel to the fibre axis, and therefore parallel to one another, will give rise to a strong equatorial reflection with a spacing equivalent to the separation of the β-sheets. This separation will depend on the nature of the amino acid residues that pack together in the intersheet space. In globular proteins these residues form part of the hydrophobic core, further increasing the thermodynamic stability of the β-sheet structures. In these proteins the separation of the β-sheets is about 10 Å, which provides a space capable of accommodating the large hydrophobic residues. However, in some fibrous β-silks, the β-strands contain high concentrations of small residues, such as serine and alanine, which reduce the intersheet separation to as little as 5 Å.

The first complete X-ray diffraction analysis of a fibrous protein with a cross-β structure was of the egg-stalk of the lacewing *Chrysopa*, by Geddes et al. [11]. The model of this insect silk proposed to explain the X-ray diffraction pattern was composed of extended polypeptide chains containing short bend regions which allowed the chains to fold back and forth to form a β-sheet ribbon about 25 Å wide and of indefinite length, whose individual β-strands were perpendicular to the long axis of the egg-stalk. These ribbons are stacked face to face with a separation of about 15 Å. It should be noted that in the *Chrysopa* model many ribbons were assumed to be present in the stack, thus forming a micellar structure consistent with the macroscopic egg-stalk, whereas a fibre as seen in amyloid would be expected to contain a specific small number of β-ribbons.

A further significant feature of the *Chrysopa* model is that the ribbons are represented as flat β-sheets, as described by Pauling and Corey [10], even though the first X-ray crystallographic studies on globular proteins reported concurrently with the Geddes model were revealing β-sheets with characteristic twists. For example, the crystal structure of an enzyme, lysozyme [12], showed that residues 42–62 form a three-stranded sheet-like structure that has many of the characteristics of the Pauling and Corey model. The only significant difference was that while the Pauling and Corey model assumed that adjacent β-strands would be exactly parallel (or antiparallel) to one another, giving rise to a 'flat' β-sheet, the adjacent β-strands in lysozyme were found to be arranged with an angle of about 15° between them, producing a twisted β-sheet. While it was possible that this was a distortion resulting from the

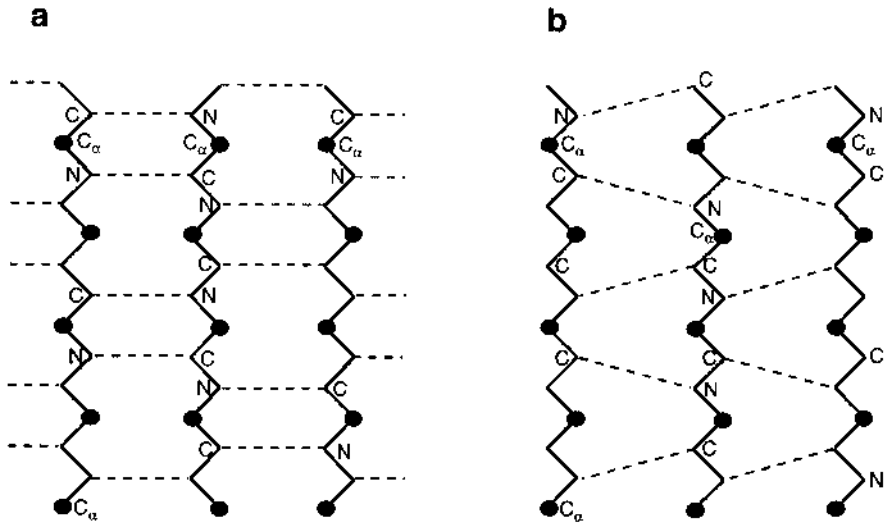

Figure 4. Schematic of β-sheet structure. Representation of hydrogen-bonding patterns in β-sheet structure, showing antiparallel (*a*) and parallel (*b*) arrangements of hydrogen bonding.

small size of the lysozyme β-sheet, in the slightly later structure of the enzyme carboxypeptidase [13] with an 8-stranded sheet, confirmed the same degree and *direction* of twist as in lysozyme. Subsequent X-ray studies on a range of globular proteins showed that β-sheet structures were common and that in nearly every case they were twisted and not flat.

The observation that β-sheets, whether parallel, antiparallel or mixed, in a variety of globular proteins, were twisted by roughly the same extent and in the same sense suggested a specific cause. The explanation was given by Chothia [14], who showed that in the flat β-sheet the CO and NH groups of the peptide groups around each Cα were too close to the atoms of the associated side-chain, and that the close contacts would be relieved by a rotation of the peptides by about 15° in the direction observed experimentally. This analysis demonstrated that for all residues, except glycine which lacks a side-chain, the twisted β-sheet is a lower energy state than the flat sheet and would be expected to occur in polypeptides with normal amino acid compositions. If the β-sheet in the *Chrysopa* silk is in fact a flat sheet, one possible explanation could be the presence of a particular sequence of glycine residues that may relieve the potential strain around α-carbon atoms. Although special patterns of glycine residues may occur in polypeptides *designed* to form biological fibres, it is unlikely to be a factor in disease-state amyloids, which are formed from proteins with sequences characteristic of normal globular folds. Because the twist occurs about an axis parallel to the fibre axis of a cross-β structure, any degree of twist will have a major effect on the description and properties of amyloid fibrils whose cross-β structures may be composed of large numbers of sequential β-strands.

X-ray diffraction studies of amyloid fibrils

Fibrous protein samples, like amyloid, are usually exposed to the X-ray beam with the long axis of the fibrils more or less perpendicular to the direction of the beam. The X-ray reflections are then distinguished by their direction with reference to the fibre axis and their distance from the centre of the pattern: *meridional* reflections are defined as those lying parallel to the fibre axis; and *equatorial* reflections are those positioned at right angles to the fibre axis (fig. 2). If the long axes of the individual fibrils within a bundle of fibrils, or the bundles themselves, deviate from the mean fibre axis, the corresponding reflections will be drawn out into arcs whose angular dispersion is related to the relative dispersion within the fibrillar bundles. Although it is advantageous to obtain diffraction data from well-aligned samples, all that is required in the first instance is for the meridional and equatorial reflections to be distinguishable from one another, which is possible in most amyloid samples.

The interpretation of X-ray fibre diffraction patterns must be informed by the idea that fibres are strictly crystalline only in the direction of the fibre axis. In directions perpendicular to the fibre axis the fibres may at best be packed in a pseudo-crystalline array, usually in an approximation of hexagonal close packing in

which neighbouring fibres are rotationally at random orientations to one another about their long axes. The effect that this has on the diffraction pattern is to give rise to the possibility of normal Bragg reflections along the meridian of the pattern, i.e. parallel to the fibre axis; but in the equatorial direction, i.e. perpendicular to the fibre axis, the reflections will be of the non-Bragg type. Burge [15, 16] has shown that for the pseudo-hexagonally close-packed fibres, the spacing of the equatorial reflections can be described by zero-order Bessel functions, dependent only on the average centre-to-centre spacing of the fibrils. The intensities of these reflections will then be related to the molecular transform of the radial electron-density distribution of an individual fibril. It is unfortunate that amyloid fibrils, although highly structured individually, do not pack together with any regularity, and as a result only a relatively basic structural interpretation can be applied to the currently available diffraction patterns. For a more detailed interpretation to be made, fibre samples of greater internal order will need to be produced. One technique that has proved useful for synthetic amyloid fibrils is to allow the fibrils to grow in intense magnetic fields ($\geq$2 Tesla), which appears to enhance their alignment and hence improve their diffraction patterns. It is, however, unlikely to be able to improve the alignment of preformed, ex vivo fibrils.

The earliest reported fibre diffraction investigations, of serum amyloid A and light-chain amyloid, reported an intense meridional reflection at 4.68 Å and an equatorial reflection at 9.8 Å [17–19]. This pattern is characteristic of the cross-β structure described above, in that the structural repeat of 4.68 Å along the fibre axis corresponds to the spacing of adjacent β-strands, and the 9.8-Å spacing perpendicular to the fibre axis corresponds to the face-to-face separation of the β-sheets. This latter, of course, can only occur if the amyloid fibrils, or protofilaments, are composed of two or more β-sheets.

The reflections at approximately 4.7 Å on the meridian and 10 Å on the equator have been seen subsequently in all amyloid fibre diffraction patterns and submit to the same interpretation, with some slight variation allowed to reflect the structural characteristics of different amyloids. For example, calcitonin fibrils grown in vitro [5], and insulin fibrils produced by heating and cooling the protein under acidic conditions, both give fibre diffraction images exhibiting strong, sharp meridional reflections at 4.76 Å and more diffuse equatorial reflections at approximately 10 Å [20]. Purified amyloid cores isolated from senile plaques associated with Alzheimer's disease show reflections at 4.76 Å and approximately 10.6 Å [21], and prion rods exhibit a prominent interstrand spacing at 4.72 Å and an equatorial spacing of 8.82 Å [6].

A significant advance in the X-ray analysis of amyloid has been achieved recently by the use of the intense X-ray beams produced by synchrotron radiation sources ([22, 23] M. Sunde, unpublished observations) whose beam flux may be up to 100 times higher than those of laboratory X-ray sources. The use of the Daresbury Synchrotron Radiation Source (SRS) in England and the European Synchrotron Facility (ESRF) at Grenoble, France, to collect data from a variety of ex vivo and synthetic amyloid fibrils has produced diffraction patterns containing families of several reflections in the meridional and equatorial directions, in place of the single reflections seen with laboratory X-ray sources (fig. 5). The most thoroughly studied amyloid fibrils to date have been those extracted from the vitreous humour from Swedish patients with FAP, composed of the Val30Met variant of transthyretin. In X-ray patterns from these fibrils taken on the Daresbury SRS, at least seven unique meridional reflections can be observed out to 2 Å resolution, and nine equatorial reflections out to about 3.5 Å resolution. This enhanced data set has provided the input for the most detailed analysis so far of the molecular structure of amyloid fibrils.

The reflections observed in the extended meridional pattern of Val30Met transthyretin amyloid [23], disclosed by the use of synchrotron radiation, are listed in table 2. If these reflections are indexed as Bragg reflections, most fit a minimum repeat distance of 28.9 Å. However, it is apparent that the expected '4.7-Å' reflection is in fact a close doublet of reflections at 4.83 Å and 4.615 Å, and this and an accurately measurable high-angle reflection at 2.02 Å do not fit this repeat distance. This suggests that 28.9 Å is probably a pseudo-repeat, and the true repeat is four times as long, namely 115.5 Å. All observable meridionals index as orders of this single repeat spacing of 115.5 Å to within a few parts in a thousand (table 2).

The nature of this meridional repeat can be determined by noting from table 2 that the intense 4.83 Å reflection, and its second order at 2.41 Å, which characterize the scattering from the β-strands in the cross-β structure, index as the 24th and 48th orders of the 115.5-Å repeat. This shows that while this new X-ray pattern is fully consistent with a cross-β type of structure (that is with β-strands arranged perpendicular to the fibre axis and hydrogen-bonded into sheets of indefinite length which run parallel to the fibre axis), the β-strands in the Val30Met transthyretin fibrils are grouped into previously unsuspected sets of 24, repeating regularly along the fibril axis. The 24-stranded repeating unit does not seem to have any obvious connection with the transthyretin molecule, which contains much smaller β-structures, and it appears to represent a structural repeating unit of a novel kind.

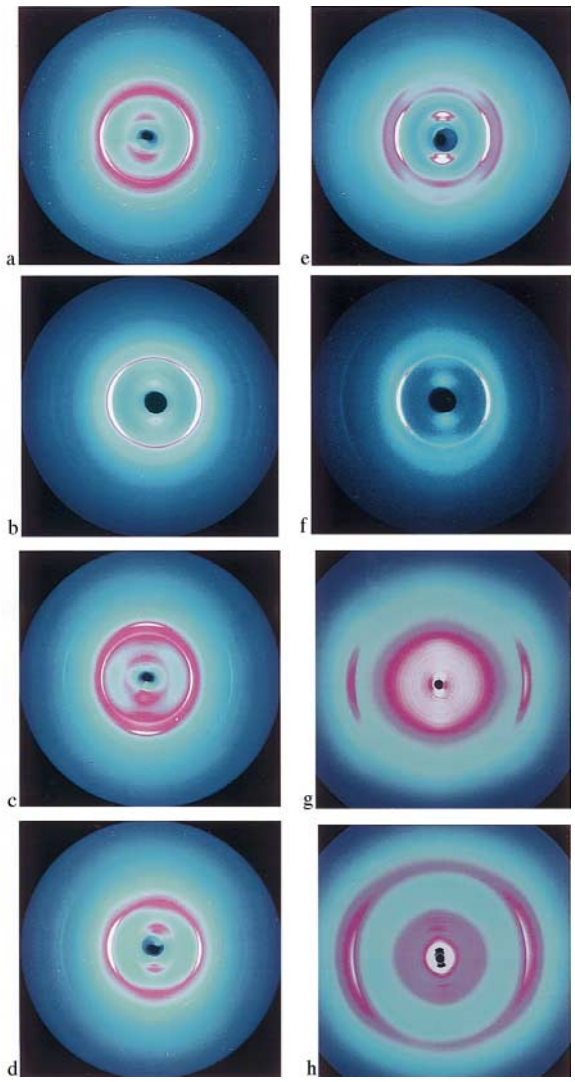

Figure 5. Collection of eight fibre diffraction patterns from various amyloids. X-ray fibre diffraction patterns from eight different ex vivo and synthetic amyloid fibril samples. The meridional axis (direction parallel to the fibril axis) is the vertical axis in this display. Amyloid fibril samples as follows: (*a*) Gly47Val transthyretin, (*b*) Val30Met transthyretin, (*c*) apolipoprotein A-1, (*d*) immunoglobulin light chain, (*e*) peptide with the sequence of the A-strand of human transthyretin, (*f*) peptide with the sequence of residues 20–29 of the islet-associated polypeptide, (*g*) serum amyloid A, (*h*) Asp67His lysozyme.

Table 2. Indices of the meridional reflections.

d (obs) Å	Index	Calculated repeat (Å)
4.83	24	115.9
4.625	25	115.6
3.860	30	115.8
3.215	36	115.7
2.880	40	115.2
2.409	48	115.6
2.022	57	115.3

The probable nature of the 24-stranded repeating unit in the transthyretin fibril is suggested by the fact that the indices of the observed meridional reflections tend to be multiples of four (hence the 28.9-Å pseudo-repeat), which is a condition indicative of the presence of a (pseudo) fourfold screw axis parallel to the axis of the protofilament. Less convincingly, the indices may be multiples of three, which would indicate a threefold screw axis. A fourfold screw axis (either left- or right-handed) requires the 24-stranded repeating unit to be composed of four equivalent six-stranded units, each related to the next by a translation of 28.9 Å (115.5 Å/4) and a rotation of 90°(360°/4). A typical six-stranded β-sheet observed in globular proteins (for example strands AGHH′G′A′ or BEFF′E′B′ of transthyretin [24]), would have a dimension perpendicular to the β-strands in the plane of the β-sheet of about 28.8 Å (6 × ca. 4.8 Å), and a twist of the sixth strand relative to the first of approximately 90°. The screw axis would therefore generate, from a typically twisted six-stranded β-sheet arranged with its β-strands perpendicular to the axis, a continuously twisted 24-stranded β-sheet in which the 24th strand is twisted by 360° relative to the 0th, around an axis parallel to the filament axis. (An identical result is obtained if the screw axis is threefold and operates on an eight-stranded β-sheet). This corresponds to a helical arrangement of β-strands in which 24 β-strands form one turn of a helix with a pitch of 115.5 Å, whose axis is parallel to the axis of the protofilament. One turn of this 'β-sheet helix', shown in figure 6, is therefore identified with the 115.5-Å repeating unit. The extension of the X-ray pattern to at least 2.0 Å along the meridian indicates that there is a high degree of crystalline order along the fibril axis which can be most easily understood if the helical hydrogen-bonded structure extends indefinitely along the fibre axis.

The classic cross-β X-ray pattern of amyloid has a single 10-Å maximum on the equator, and this reflection has been interpreted as representing the spacing of β-sheets perpendicular to the fibril axis. The equatorial reflections observed from the X-ray patterns of Val30Met transthyretin fibrils contain a number of diffraction maxima (table 3). The spacings of the equatorial reflections can be interpreted in terms of 'non-Bragg maxima' arising from short-range lateral order within the amyloid fibrils [15] composed of protofilaments with a centre-to-centre spacing of 65 Å observed in electron micrographs [8]. The *intensities* of the equatorial reflections can be interpreted as arising from the overall molecular structure of the protofilaments as projected down their long axis.

Table 3. Spacings of the equatorial reflections.

d (obs) Å	Relative intensity
64	vs
34	s
20.2	vw
12.6	m
10.1	m
7.56	vw
6.05	w
5.32	m
3.94	s

s: strong; vs: very strong; m: medium; w: weak; vw: very weak.

The diameter (65 Å) of the protofilament in the model of transthyretin amyloid [23] is very similar to the dimension of the cross-section of the TTR molecule in the direction perpendicular to its β-strands (50 Å $\times$ 70 Å) [24]. This suggests that they are formed from the same *number* of β-sheets, namely four (fig. 6). Intensity distributions, calculated with the assumption that the scattering occurs predominantly from the β-sheets (which are represented by two thin co-axial cylinders of radius 6.5 Å and 16.5 Å), produce peaks at 10 Å and at 5 Å. These results are in reasonable agreement with the major features of the observed intensity distribution.

This helical structure composed of a continuous β-sheet has not been reported before. It is however evident that the limited β-sheets that occur in many globular proteins form partial helical structures which are in fact short segments of complete helical turns that seem to occur in amyloid. The reason for the partial nature of the 'β-sheet helices' in globular proteins is that these molecules are not large enough to contain a 24-stranded β-sheet which is needed to develop a complete turn of the helix described for the amyloid fibril. Examination of the illustrations of globular proteins produced by Richardson [25], will show that in many proteins of the α/β type, the strands of the internal β-sheet are related to one another by a rotation of approximately 15° about an axis that is perpendicular to the β-strands and in the plane of the sheet. Because the number of β-stands in these molecules is normally in the range of 6–9, the sheets describe no more than 1/4 to 1/3 of a helical turn, but extension of the number of β-strands would allow the development of complete helical structures of essentially the type described for amyloid. The only significant difference between the complete β-sheet helix described for amyloid [23], and the partial β-sheet helices found in many globular proteins, is that the helix axis is moved from the plane of the β-sheets in globular examples to a position between face-to-face pairs of β-sheets in amyloid, a distance of about 5 Å. This small distortion may parallel the case of α-helical coiled coils, where in order to allow two α-helices to form a super-

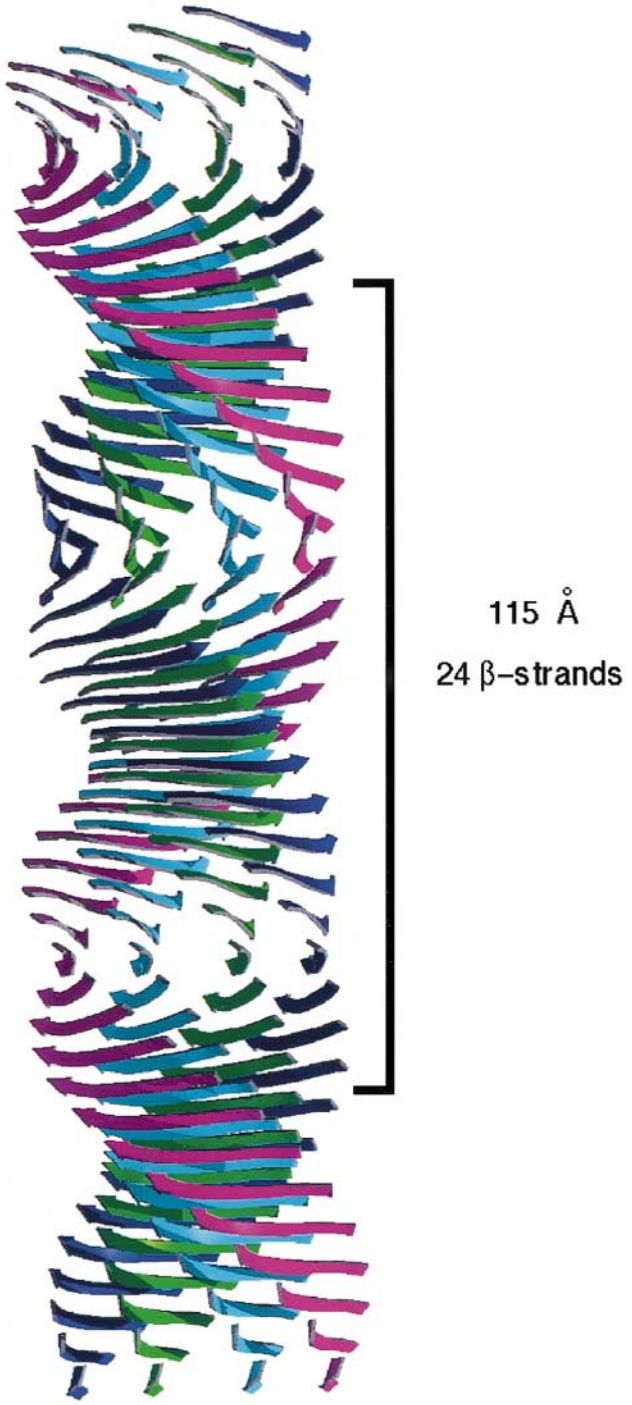

Figure 6. Model of the amyloid fibril structure core. Molecular model of the common core protofilament structure of amyloid fibrils. A number of β-sheets (four illustrated here) make up the protofilament structure. These sheets run parallel to the axis of the protofilament, with their component β-strands perpendicular to the fibril axis. With normal twisting of the β-strands, the β-sheets twist around a common helical axis which coincides with the axis of the protofilament, giving a helical repeat of 115.5 Å containing 24 β-strands. The direction of arrows in this figure is not intended to represent chain directionality. The fibre diffraction data indicate that the β-sheets in amyloid probably contain a mixture of parallel and antiparallel hydrogen-bonded β-strands, but the relative proportions cannot be determined. Image produced with the program Molscript [73].

coil, the normally straight helices curve around a common helical axis lying between them, causing a small local distortion to the helical structures which is more than compensated by the favourable energy of interaction in the coiled coil.

The most interesting consequences of the β-sheet helix structure proposed for amyloid is first that it reconciles the fibril structure with the twisted β-sheet. This is particularly important because the analysis carried out by Chothia [14] shows that for proteins of normal amino acid sequence the twisted β-sheet is of lower energy than the flat sheet. Therefore the twisted sheet would be expected for amyloid fibrils, which are known to form spontaneously from many oligopeptides and denatured proteins, and where high stability of the fibrils, once formed, is a major factor of their disease-forming properties. A second major consequence is that the β-sheet helix allows a continuous pattern of β-type hydrogen bonds to link the peptides along the complete length of the fibril, which may be many thousands of angstrom units. This structure would be expected to result in straight, well-defined fibrils, with a high degree of stability, as is observed (fig. 1).

A common core structure for amyloid fibrils

The detailed model of the core structure of the Val30Met transthyretin amyloid fibril presented above was determined from an interpretation of the features of the high-resolution X-ray diffraction pattern. Knowing the significance of each feature of the diffraction pattern enables the structures of amyloid fibrils from different sources to be compared through their X-ray diffraction patterns. Recently, the intense X-ray beams from synchrotron radiation sources have been used to investigate the molecular structure of a variety of amyloid samples (M. Sunde, unpublished observations), including ex vivo fibrils from patients with immunoglobulin light chain, serum amyloid A, apolipoprotein A-1, transthyretin (two different variants), and lysozyme amyloidoses and synthetic amyloid fibrils formed from amyloidogenic fragments of transthyretin and the islet-associated polypeptide. The high-resolution diffraction images collected from the various amyloid fibrils are illustrated in figure 5.

All of these fibril samples give cross-β X-ray diffraction patterns with the major features which have been reported for other amyloids, as described above, but the use of synchrotron radiation extends the observable diffraction on the meridian to below 2 Å in some samples and allows detailed analysis of the meridional diffraction patterns and indexing of these reflections. This work reveals that in spite of the large differences in the size and structures of the polypeptide precursors of the fibrils, the similarities in the diffraction patterns are very marked. This indicates that different amyloid fibrils actually share a common molecular skeleton on the fibril axis, with the same atomic spacings.

In all of the diffraction images from different amyloids, the meridional diffraction pattern is dominated by an intense reflection at approximately 4.7 Å which derives from the mean separation of the hydrogen-bonded β-strands which are arranged perpendicular to the fibre axis in the cross-β structure. In addition to this intense reflection, the synchrotron radiation also reveals a series of weaker, higher-angle reflections, including a second order of the ca. 4.7-Å spacing. In some of the amyloid samples (fig. 5, a to d), the intense '4.7-Å' reflection can be seen to be a close doublet, with components at 4.82 Å and 4.63 Å. In patterns where this doublet cannot be resolved, its presence can be inferred from the observation that the calculated first order of the second harmonic of the '4.7-Å' spacing, found at 2.39–2.41 Å, maps to the extreme inner edge of the intense '4.7-Å' reflection, leaving space for a 4.6-Å component within the overall intensity envelope. The weaker, higher-angle reflections occur at closely similar spacings in the different samples. For example, reflections at 2.39–2.41 Å (the second order of the intense 4.82 Å) and reflections with spacings of 3.2 Å, 2.8–2.9 Å, 2.22–2.27 Å and 2.00–2.02 Å occur frequently. Since these latter reflections are very weak, even in relatively well-oriented patterns, their absence from certain images may simply indicate that they are too weak to be observed above the noise level in those patterns.

The observed meridional spacings from all of these different samples can be fitted to the same repeat distance, 115.5 Å, which is that which has been observed in the diffraction from Val30Met transthyretin (table 2). This similarity in the diffraction over the medium- and high-angle regions of the meridional X-ray pattern can only occur if the fibrils have well-defined and closely similar molecular structures, at least insofar as their ordered core components are concerned. The implication of this is that all amyloid fibrils have as their core structure the continuous β-sheet helix (fig. 5) that has been described in detail for the transthyretin amyloid fibril [23].

A model of the amyloid protofilament, containing helically twisted β-sheets, gives reasonable agreement with the major features of the fibre diffraction patterns exhibited by all amyloid fibrils so far examined. Within this framework there are many possibilities for fibrils to be composed of different numbers or arrangements of protofilaments and for those protofilaments to vary in diameter as a result of the need to incorporate different-sized loops linking the β-strands. It is also possible that some amyloids may be composed of only one pair of β-sheets rather than the two pairs of sheets thought to compose the transthyretin amyloid protofilament. In spite of the possibility of these considerable variations,

the common core structure indicated by the synchrotron diffraction patterns is evidence that amyloid fibrils do have a well-defined generic molecular structure that accounts for their characteristic disease-forming properties.

X-ray studies of amyloidogenic proteins

Proteins that are responsible for amyloid disease are quite varied, as is the form in which they are incorporated into fibrils. In some proteins such as insulin, β_2-microglobulin and transthyretin (in senile systemic amyloidosis) the complete wild-type polypeptide chains appear to be involved. More often it is found that it is severely truncated polypeptide chains of normal proteins, such as in the Aβ protein of Alzheimer's disease, apolipoprotein AI and gelsolin, that form the amyloid. In others, the amyloid fibrils are found to be associated with specific amino acid variants of normal proteins. A particularly striking example of this concerns the plasma protein transthyretin, where more than 50 different amyloidogenic variants have been reported as giving rise to amyloidoses. In this protein, therefore, variation of at least 40% of the residue positions in the polypeptide chain results in amyloid formation. Another example involves the much-studied enzyme lysozyme, where two specific single amino acid variants have been associated with lethal, familial amyloidoses. As the structure and behaviour of the two latter proteins have been well characterized, they have been used to study the molecular processes involved in fibril formation and growth.

Transthyretin variants which form amyloid

The plasma protein transthyretin (TTR), formerly known as prealbumin, forms the amyloid in senile systemic amyloid (SSA), where the wild-type protein is deposited in fibrils, and in FAP, where variant transthyretin chains are involved. More than 50 different FAP variants of TTR have now been listed by Saraiva [26]. FAP is an autosomal dominant disease affecting kindreds predominantly in Portugal, Sweden, Japan and the USA. The clinical features of the disease include peripheral neuropathy, cardiac dysfunction and in some cases vitreous opacities. A transthyretin variant which causes amyloid deposition in the brain with the symptoms of dementia, but not neuropathy, has also been described recently [27]. Approaches to understanding how the amino acid variants of TTR might predispose the protein to form amyloid fibrils have included the X-ray analysis of crystals of specific amyloidogenic variants of TTR, and statistical analyses of potential amyloidogenic characteristics in all 50 known FAP variants of TTR. Although these studies are far from conclusive, some indications of the molecular basis of amyloid formation are starting to appear.

The crystal structures of several different FAP transthyretin variants have been solved [28–31] and compared with the crystal structure of the wild-type protein (fig. 7). The crystal structures of Val30Met transthyretin [28–30] show that the overall structure of the tetramer is maintained. One study of this variant [29] has indicated that the effect of the substitution of the bulkier residue methionine for valine at an internal site is to produce changes in the hydrophobic core of the protein which are transmitted through the core to displace parts of sequentially distant regions of β-strands A and D. The changes result in a substantial modification of the interaction between residues 10 and 52 and apparently place Cys10 in a more exposed

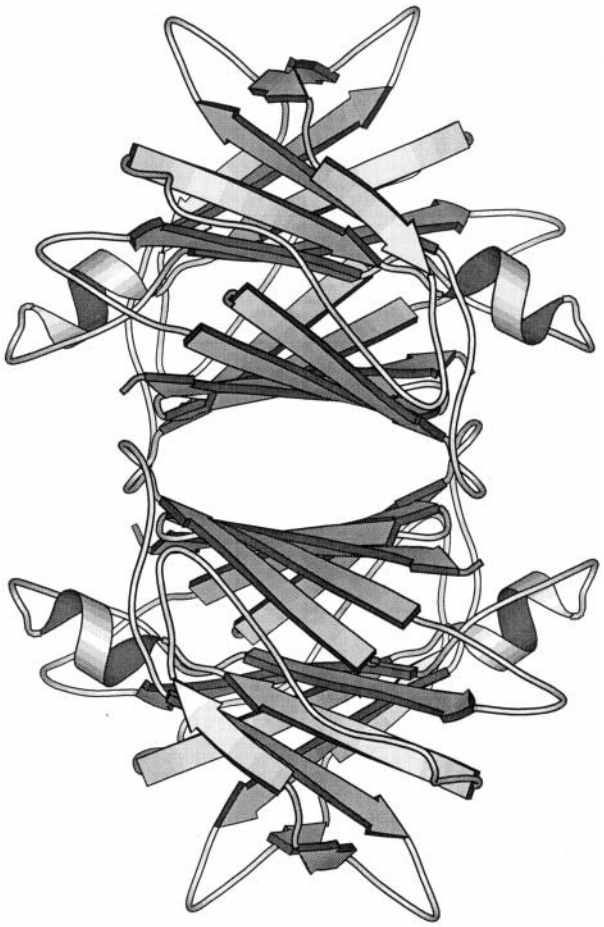

Figure 7. Ribbon diagram of the transthyretin tetramer. View of the transthyretin tetramer, along the axis of the ligand-binding channel. The 55-kDa homotetramer is the biologically active form of the protein, with the monomers associating in such a way as to generate a stack of four 8-stranded β-sheets with a large central channel through the protein which is the site for thyroid hormone binding. Image produced with the program Molscript [73].

position, where it is possible that it may participate in a disulphide bond with another transthyretin molecule. The presence of disulphide bonds between transthyretin molecules has been detected in amyloid fibrils [32] but has been shown not to be necessary for amyloid fibril formation [33]. A second study [29] has detected changes of approximately 1 Å in the relative positions of the four β-sheets in the TTR, which may suggest a destabilization of the TTR tetramer. An equivalent analysis of the Val122Ile variant of TTR [34] indicates a lengthening of the hydrogen bonds in some intersubunit hydrogen bonds, which may also be consistent with the destabilization of the tetrameric structure of TTR.

Although no correlation of amyloidogenicity with a variety of 'bulk' properties, such as size, charge, hydrophilicity, and internal or external location, of the residue substitutions in the 50 FAP variants listed by Saraiva [26] could be made, a significant correlation seems to exist with the location of the variants along the polypeptide chain [35, 36]. Standard frequency analysis of the residue positions of the amyloidogenic mutations shows a significant mutational 'hot spot' in the region of residues 45–55. In the three-dimensional structure of TTR [24] this segment of the polypeptide chain occurs on the outside of the molecule which includes the β-strands C and D and the intervening C-D loop. The two β-strands correspond to the edges of the two large β-sheet pairs that form the structural framework of the TTR molecule. The amyloidogenic variants in this region are such as to potentially disturb or disrupt the molecular structure of these 'edge' β-strands. Mapping all of these mutations onto the three-dimensional structure of transthyretin shows that some of the mutations that are situated at a distance from the C-D region on the polypeptide chain may have indirect effects via side-chain clashes with C-D strand residues [35, 36]. For example, as described above, the effect of the methionine for valine substitution at position 30, the most common FAP variant, is observed to be transferred through the protein core to residues 56–58 which form β-strand D [29]. Recombinant transthyretin proteins with triple substitutions at residues 56–58, or with a triple deletion at this site, have been shown to be spontaneously amyloidogenic [36]. Serpell et al. [35] and Kelly and Lansbury [37] have proposed that the three residues of the short D-strand are susceptible to disruption of their higher-order structure and in solution can allow the D-strand to be displaced to expose the longer A-strand to possible hydrogen-bond interaction with the A-strand of another transthyretin molecule, in a manner which would lead to aggregation and fibril formation. In this model the A-strand would be the 'amyloidogenic determinant', whose exposure in the substituted D-strand variants would represent the triggering process of amyloid formation. Such a model would also be fully consistent with the location of the hot spot in the region.

There also appears to be a correlation between transthyretin tetramer stability and amyloidogenicity, and between the affinity for thyroxine and amyloidogenicity, and this may be exploited to inhibit TTR fibril formation [38]. As the thyroxine-binding sites are only generated in the TTR tetramer, thyroxine-binding affinity may be a sensitive index of the stability of quaternary structure. A comparison of the thyroxine-binding affinities of 10 different human transthyretin variants [39] has shown that binding affinities for thyroxine vary in the following manner (strongest binding to weakest) $\text{Ala109Thr}_{\text{het}} > \text{wild type} = \text{Thr60Ala}_{\text{het}} = \text{Val122Ile}_{\text{het}} > \text{Leu58His}_{\text{het}}$ $\text{Ser77Tyr}_{\text{het}}$ $\text{Ile84Ser}_{\text{het}}$ $\text{Val122Ile}_{\text{hom}}$ $\text{Val30Met}_{\text{het}} \gg \text{Val30Met}_{\text{hom}}$. This series reflects the relative aggression of the mutations. The crystal structures of various transthyretin variants support the hypothesis that reduced thyroxine affinity, as a consequence of structural changes, is correlated with reduced tetramer stability and increased amyloidogenicity. The changes in the inner sheet of the Val30Met variant [29], which cause a decrease in the width of the thyroxine-binding channel of 0.3 Å, may be the reason for the reduced thyroxine affinity displayed by this variant. The non-amyloidogenic Ala109Thr transthyretin variant [30], which displays an affinity for thyroxine that is three times higher than that shown by the wild-type protein, displays a wider entrance to the thyroxine-binding channel. Saraiva and co-workers have solved the crystal structures of Thr119Met, Leu55Pro and Val122Ile transthyretins [31]. The Met119 substitution is one which appears to have protective or 'non-amyloidogenic' properties. The substitution of Met for Thr at position 119 has an effect on the binding affinity for thyroxine, which is increased 1.5- to 2-fold over that of the wild-type protein. In the Leu55Pro protein, the position of the D-strand of the molecule is altered, in accordance with the 'hot-spot' hypothesis of Serpell et al. [35, 36] and the proposal of Kelly and Lansbury [37], which suggested that the conformation of this region of the monomer is important in fibril formation. It is also interesting that this variant has virtually no affinity for thyroxine, suggesting that the stability of the tetramer may be so reduced in solution as to render it incapable of stable thyroxine binding.

These data seem to suggest that for amyloid formation involving TTR to occur, two separate requirements must be fulfilled: the disruption of the D-strand and the destabilization of the tetramer. It seems possible to account for these two factors in a single model of amyloidogenesis in TTR. In this model the A-strand would be the 'amyloidogenic determinant', whose exposure on substitution of the D-strand would represent the triggering process of amyloid formation. On the basis that the changes in tertiary structure implied by the disruption of the D-strand may be transmitted to

the tetramer interfaces, it is not unreasonable to expect the amyloidogenic variants to destabilize the tertiary structure of TTR to some extent. In this case the TTR monomer with its amyloidogenic determinant exposed would form the building block for the FAP amyloid fibril. It has been shown independently [23] that the TTR tetramer cannot be a building block for FAP amyloid. Such a model would also be consistent with the location of the hot spot in the region from the analysis of all FAP variants [36], the structural changes in individual variants mapped in the crystallographic studies [28–34], and the chemical and biophysical studies [37, 38, 40]. It should be noted that there is no reason to believe that this model is appropriate to amyloidogenesis in any protein system other than TTR; a quite different mechanism is proposed for lysozyme (see below).

Figure 8. Comparison of wild-type and amyloidogenic variant lysozyme structures. Overlay of ribbon diagrams representing the structures of wild-type human lysozyme (grey) and the soluble form of Asp67His lysozyme (black). The large changes in the β-domain of the Asp67His protein are clearly seen. Disulphide bridges are shown with dotted lines. The Ile56Thr variant human lysozyme has a native structure almost indistinguishable from that of wild-type human lysozyme. Image produced with the program Molscript [73].

Lysozyme variants which form amyloid

The identification of Ile56Thr and Asp67His variant human lysozymes as the fibril proteins in amyloid deposits was the first report of a lysozyme-associated disease [41]. The two variant lysozymes identified in amyloid deposits have single amino acid mutations, either threonine for isoleucine at position 56 or histidine for aspartate at position 67, and both substitutions occur at highly conserved positions in the sequence. Human lysozyme has been extensively studied; the monomeric wild-type protein folds cooperatively with a two-state mechanism, into two domains, with the active site formed in the cleft between the mainly helical α-domain and the β-domain which is made up of a triple-stranded β-sheet and a long loop [42–45].

High-resolution X-ray studies [46] show that the crystalline forms of the Ile56Thr and Asp67His molecules have wild type-like folds; however, there are large differences in the chain conformation in the β-domain of the Asp67His variant compared with wild-type and Ile56Thr lysozyme (fig. 8). Aspartate67 plays a central role in the network of hydrogen bonds that stabilizes the β-domain of wild-type human lysozyme, and substitution of this residue by histidine results in a concerted movement of the β-sheet and the long loop within the β-domain away from each other, distortion of the active site and an overall displacement of some backbone atoms from wild-type positions by 11 Å.

The key to both amyloidogenic mutations in human lysozyme apparently lies in the effect they produce at the interface between the α- and β-domains, where residue 56 acts as an anchor of the β-domain onto the α-domain. In the Asp67His variant, the changes in the orientation of the β-domain and long loop are transmitted to residue 56, resulting in an altered side-chain orientation and an increased β-factor, in Ile56 relative to the wild-type enzyme ($8.8 \rightarrow 12.0$). A similar, increased B-factor (12.3) is found for Thr56 in the other variant, where this hydrophilic side-chain is in an unfavourable environment. The base of the β-domain appears to be more mobile in the variants than in the wild-type protein, and domain adhesion may be weakened. Docking of the β-domain onto the α-domain is required for lysozyme to achieve its rigid, native fold [45], so the two mutations act on a region which is crucial for stability of the native, folded protein.

Both variants are less thermostable than the wild-type protein, with midpoints of denaturation approximately 12 °C lower than that of the wild-type protein at pH 5.0 [46]. More significantly, however, the unfolding transition of the two amyloidogenic variants, while reversible under conditions in which fibril formation does not occur, is non-cooperative. This results in a partially folded state being significantly populated near the midpoint of unfolding. In contrast to the wild-type protein, which displays a core of amide hydrogens in the α-domain which are protected against hydrogen exchange, the two amyloidogenic variants do not show protection of any amides, behaviour that indicates that the alterations in the domain interface of the Ile56Thr and Asp67His variants reduce the stability and cooperativity

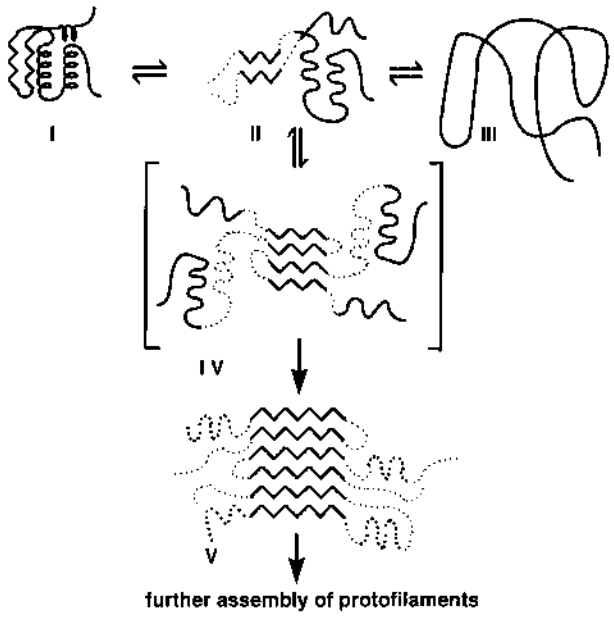

Figure 9. Proposed mechanism for lysozyme amyloidosis. A partially-folded, molten globule-like form of the protein (II), distinct from the native (I) and denatured (III) states of the protein, self-associates through the β-domain (IV) to initiate fibril formation. This provides the template for further deposition of protein and for the development of the stable, mainly β-sheet, core structure of the fibril (V). The dotted chain in II and IV indicates unfolding of the chain from its native conformation. The dotted segments in V represent the possibility that not all of the polypeptide sequence is involved in the cross-β structure; the nature of this residual structure is not known.

of the native fold such that both the amplitude and frequency of the native state fluctuations are increased, even at 37 °C, to an extent that allows access to the interior of the protein. The transient population of the amyloidogenic proteins in a molten globule-like state which lacks global cooperativity could facilitate the structural conversion from the globular form observed in the crystals to the fibrillar form present in amyloid deposits (fig. 9).

Biological implications of the structural studies

The origins of the different amyloidoses appear quite diverse, with some arising from a genetic mutation, others apparently from polypeptide misprocessing or from an unusual accumulation of full-length wild-type protein. From the short peptide cleavage products of larger proteins, e.g. the Alzheimer's Aβ peptide and the islet-associated polypeptide which forms amyloid in Type II diabetes, to full-length proteins such as the prion protein, lysozyme and transthyretin, the proteins and peptides known to form amyloid fibrils cover a range of structure and function.

The nature of the polypeptide component of the fibrils is used to define the type of amyloidosis, and it affects the pathology of the disease state, yet all amyloid fibrils, regardless of the character of the precursor or the site of deposition in the body, appear to have a related ultrastructure and a closely similar molecular core structure.

The closely similar cross-β fibre diffraction patterns exhibited by amyloid fibrils indicate that this underlying ordered structure is primarily β-sheet, with the constituent β-strands lying at right angles to the fibre axis. Many of the amyloid precursors have major helical components in their active globular forms. The native structures of proteins such as insulin [47], whose wild-type sequence is amyloidogenic, and cystatin [48] and gelsolin [49], which have cleavage products which form fibrils, display extensive elements of helical structure. The NMR structure of the prion protein domain [50] has shown that it is predominantly helical, and the structure of apolipoprotein A-1 is predicted to be mainly helical [51]. Even those proteins such as the immunoglobulin light chain [52], transthyretin [24] and β_2-microglobulin [53], which have mainly β-sheet native folds, could not aggregate without a structural transition to produce a cross-β fibril that would generate the characteristic diffraction pattern [23]. As discussed earlier, the crystal structures of several amyloidogenic transthyretin variants [28, 29, 31] and of the two lysozyme variants [46] have been solved, and all show molecular structures similar to those of the wild-type proteins, indicating that these protein sequences do encode stable tertiary folds. The implication of this is that the amyloid precursor proteins must undergo a significant structural conversion when they are deposited in the amyloid fibril. Evidence from lysozyme amyloid suggests that the amyloidogenic potential of a polypeptide is related to its conformational plasticity [46].

Studies of various fragments of the Aβ peptide have shown that the secondary structure of the peptide is dependent on the solution conditions [54–57] and that the peptide undergoes conformational changes depending on the environment. Kirshenbaum and Daggett [58] have used molecular dynamic simulations to test the possibility of helix-to-coil and helix-to-sheet transitions in the 1–28 fragment of the Aβ peptide, and they find that pH is an important factor in initiating the transition. Barrow and co-workers [59] have induced an α-helix to β-sheet transition in 1–39 and 1–42 Aβ peptides, and Terzi et al. [60] have demonstrated a random coil-to-β sheet transition in fragment 25–35.

Similar structural transitions are observed within the prion protein. Fourier Transform Infra-Red data show that the prion protein has 40% helix in the cellular form [61]. This is in agreement with secondary structure predictions [62] and the NMR structure of the prion domain [50], yet the infectious form of the protein has

43% β-sheet and only 30% helix, and three of the four peptides corresponding to the helical segments adopt a β-sheet conformation in solution [63]. The β-sheet content of the prion protein appears to be related to its 'infectivity' [64]. Cohen and co-workers have suggested a model whereby a partially folded monomer of the prion protein is an intermediate between the cellular form and the scrapie form [65], and there is evidence that prion amyloid is an aggregate of a molten globule-like intermediate [66]. The scrapie form may be able to act as a template for the conversion of the intermediate into the insoluble form [65].

Kelly and co-workers have also shown that transthyretin undergoes a pH-mediated tetramer-to-monomer transition in the pH range where amyloid formation occurs and that this involves a conformational change [38, 40, 67, 68]. Even in this predominantly β-sheet protein some structural transition must take place to form a rearranged tetramer or monomeric intermediate that is the building block of the amyloid fibril [23].

Taking into account the range of proteins and peptides that can form amyloid, the process of amyloidogenesis must involve large-scale structural conversion. This is most clearly demonstrated by the involvement of predominantly α-helical proteins, such as lysozyme, in amyloid fibril formation. It also underlies the mechanism of 'infection' in the prion diseases, where the scrapie form of the prion protein appears to convert the mainly α-helical cellular form into β-structure. Amyloidogenic counterparts of normal globular proteins often exhibit soluble molecular structures so similar to the wild types that it must be considered that it is events in abnormal folding or processing pathways that lead to amyloid formation and the deposition of this particularly stable cross-β fibrillar structure.

The transmissible spongiform encephalopathies

The most remarkable of the diseases associated with amyloid are the spongiform encephalopathies which are transmissible, both within a single species and also in certain circumstances across species barriers [69, 70]. Diseases of this type are exemplified by bovine spongiform encephalopathy (BSE), which appears to have been transmitted to cattle by feeding them the remains of sheep suffering the long-known equivalent ovine disease, scrapie. Thereafter BSE spread widely through the dairy herds in the United Kingdom, apparently by both horizontal (sheep-to-cow or cow-to-cow) and vertical (cow-to-calf) transmission. By entering the human food chain BSE is thought to be the most likely source of a new variant of Creutzfeldt-Jakob disease (CJD), a natural low-level sporadic brain disease in humans. Transmission of BSE to a number of species has been achieved experimentally by direct injection of the BSE agent into the brain, and CJD is itself thought to be transmissible within humans as exemplified by the similar disease, known as kuru, in certain tribes in New Guinea which practise the cannibalism of the (infected) brains of their ancestors. What marks out the transmissible spongiform encephalopathies is the likelihood that the transmissible agent is not an organism but a protein molecule [69]. The best evidence we have on the nature of the BSE agent is the identification of an unusual form of a protein known as a prion, which is a normal brain protein though of unknown function. The major difference between the cellular, soluble form of wild-type prion (PrPC) and the so-called scrapie form (PrPSc) is that the PrPSc has a significantly greater proportion of β-sheet in its molecular structure [63] and that it forms amyloid [69, 70].

The concept that an infective agent in a lethal disease can in certain circumstances be a protein molecule is sufficiently radical that it requires positive identification of the protein molecule and the molecular processes involved in infectivity before it can be totally accepted [68]. The evidence suggesting that the scrapie/BSE agent is not an organism derives first from the inability to demonstrate an organism with the appropriate infectivity after a long and intensive search (more than 30 years in the case of scrapie). The evidence that the agent may be a protein molecule derives from the experimental observation that the infectivity survives treatment (such as irradiation and treatment with nucleases) that normally destroys DNA, and to the identification of an altered state of the prion protein in diseased tissue. Although the involvement of the prion, or indeed any other protein, as the transmissible agent explains the absence of a DNA-dependent agent, it brings to the fore some implications about the properties and behaviour of the protein agent which are difficult for many to accept.

One difficulty is with the exceptional stability of the agent evidenced by a temperature of 200 °C required for the effective destruction of BSE infectivity in a cow's carcass. This is much higher than the denaturation temperature for normal proteins, and would seem to presuppose some unusual structural features in a moderately sized protein molecule such as the prion. The NMR structure of a fragment of the prion protein, determined by Riek and co-workers [50] does not demonstrate a molecular structure suggesting such exceptional stability.

A second difficulty is with the idea that a scrapie form of the prion molecule (PrPSc) is capable itself of directly converting many molecules of the normal cellular form of the prion to the PrPSc form in a kind of catalytic conversion [71, 72]. Although the PrPSc appears to have a greater degree of β-structure in its molecular structure than the normal, cellular form of the prion

protein, the proposal that PrPC monomers can be permanently converted to the PrPSc form through the mediation of a PrPC:PrPSc dimer, which then breaks down into PrPSc monomers thereby starting a chain reaction [65], is difficult to sustain. Even accepting the possibility that the proposed structural conversion could take place in a protein dimer, it is not easy to understand why the PrPC form is not re-established when the dimer breaks up, which would thereby inhibit any chain reaction.

It may, however, be possible to define the nature of the BSE agent which, while keeping its proteinaceous character, seems to avoid the difficulties outlined above. One characteristic of the PrPSc molecule is its ability to form amyloid fibrils. Although there is no clear evidence that PrP amyloid is itself the causative agent of BSE, the properties of the PrP amyloid make it a plausible potential candidate for the infective agent. The high-resolution X-ray diffraction analysis of the molecular structure of FAP amyloid [23] using synchrotron radiation, described above, shows that the amyloid fibrils are composed of continuous β-sheet structures, probably in a helical form, that potentially run the full length of the fibril. Further synchrotron analysis of a range of ex vivo amyloids from different diseases and precursor proteins show the same diffraction pattern as is seen in FAP, suggesting a common structure for all amyloid fibrils independent of the nature of the protein precursor (M. Sunde, unpublished observations). This is consistent with the information available from the relatively low resolution X-ray data on BSE amyloid so far observed.

If the PrPSc amyloid were the infective agent in BSE, either as complete fibrils or small fibril fragments, the great stability of the agent and also its ability to convert normal prion molecules to the scrapie form are easier to understand. With regard to stability, the extensive inter- and intramolecular hydrogen bonding in the continuous β-sheet structures would lead to great stability of the amyloid fibril, and would almost certainly give a much enhanced thermal stability as compared with the prion monomer. The conversion of α-structures to a β-form and their subsequent stable incorporation in a β-rich amyloid fibril has been demonstrated for lysozyme and the Aβ peptide, and suggests that a prion amyloid fibril could act as an effective agent to convert prion monomers into the β-rich PrPSc form by incorporating them into the growing fibril. Given the great stability of amyloid fibrils it does not seem implausible for fibrils or fragments of fibrils to survive the passage from one animal to another, or indeed from one species to another, there to continue to act as an agent for the conversion of normal prions to the scrapie form and hence pass the disease to the new host. If we consider the addition of monomers to a growing fibril as a one-dimensional crystallization process, then the transmission of the BSE/scrapie disease is akin to the implantation of a crystal 'seed' in the new animal.

Acknowledgements. The authors are grateful for the financial support from the UK Medical Research Council and the Biomed Programme of the European Union. They also acknowledge the generous collaboration of Professor Mark Pepys, Dr Paul Fraser, Dr Margarida Damas, and Professor Erik Lundgren.

1 Cohen A. S. and Calkins E. (1959) Electron microscopic observation on a fibrous component in amyloid of diverse origins. Nature **183:** 1202–1203
2 Shirahama T. and Cohen A. S. (1967) High resolution electron microscopic analysis of the amyloid fibril. J. Cell Biol. **33:** 679–706
3 Cohen A. S., Shirahama T. and Skinner M. (1981) Electron microscopy of amyloid. In: Electron Microscopy of Protein, vol. 3, pp. 165–205, Harriss, I. (ed.), Academic Press, London
4 Kirschner D. A., Abraham C. and Selkoe D. A. (1986) X-ray diffraction from intraneuronal paired helical filaments and extra-neuronal amyloid fibres in Alzheimer's disease indicates cross-β conformation. Proc. Natl. Acad. Sci. USA **83:** 503–507
5 Gilchrist P. and Bradshaw J. (1993) Amyloid formation by salmon calcitonin. Biochim. Biophys. Acta **1182:** 111–114
6 Nguyen J. T., Inouye H., Baldwin M. A., Fletterick R., Cohen F. E., Prusiner S. B. et al. (1995) X-ray diffraction from scrapie prion rod and PrP peptides. J. Mol. Biol. **252:** 412–422
7 Fraser P. E., Nguyen J. T., Surewicz W. K. and Kirschner D. A. (1991) pH dependent structural transitions of Alzheimers amyloid peptides. Biophys. J. **60:** 1190–1201
8 Serpell L. C., Sunde M., Fraser P. E., Luther P. K., Morris E., Sandgren O. et al. (1995) The examination of the structure of the transthyretin amyloid fibril by image reconstruction from electron micrographs. J. Mol. Biol. **254:** 113–118
9 Astbury W. T., Dickinson S. and Bailey K. (1935) The X-ray interpretation of denaturation and the structure of the seed globulins. Biochem. J. **29:** 2351–2360
10 Pauling L. and Corey R. (1951) Configuration of polypeptide chains with favoured orientation around single bonds: two new pleated sheets. Proc. Natl. Acad. Sci. USA **37:** 729–739
11 Geddes A. J., Parker K. D., Atkins E. D. T. and Beighton E. (1968) "Cross β" conformation in protein. J. Mol. Biol. **32:** 343–358
12 Blake C. C. F., Kornig D. F., Mair G. A., North A. C. T., Phillips D. C. and Sarma V. R. (1965) Structure of hen egg-white lysozyme. A three dimensional Fourier synthesis at 2 Å resolution. Nature **206:** 757–761
13 Reeke G. N., Hartsuck J. A., Ludwig M. L., Quiocho F. A., Steitz T. A. and Lipscomb W. N. (1967) The structure of carboxypeptidase A, VI. Some results at 2.0 Å resolution and the complex with glycyl-tyrosine at 2.8 Å resolution. Proc. Natl. Acad. Sci. USA **58:** 2220–2226
14 Chothia C. (1973) Conformations of twisted β-sheets in proteins. J. Mol. Biol. **75:** 295–302
15 Burge R. E. (1959) X-ray scattering by bundles of cylinders. Acta Crystallogr. **12:** 285–289
16 Burge R. E. (1963) Equatorial X-ray diffraction by fibrous proteins: short range order in collagen, feather keratin and f-actin. J. Mol. Biol. **7:** 213–224
17 Eanes E. D. and Glenner G. G. (1968) X-ray diffraction studies on amyloid filaments. J. Histochem. Cytochem. **16:** 673–677
18 Bonar L., Cohen A. S. and Skinner M. (1967). Characterization of the amyloid fibril as a cross-β protein. Proc. Soc. Exp. Biol. Med. **131:** 1373–1375
19 Glenner G. G., Eanes E. D. and Page D. L. (1972) The relation of the properties of congo red-stained amyloid fibrils to the β-conformation. J. Histochem. Cytochem. **20:** 821–826
20 Burke M. J. and Rougvie M. A. (1972) Cross-β protein structures I. Insulin Fibrils. Biochemistry **11:** 2435–2439

21 Kirschner D. A., Inouye H., Duffy L., Sinclair A., Lind M. and Selkoe D. A. (1987) Synthetic peptide homologous to β-protein from Alzheimer's disease forms amyloid-like fibrils in vitro. Proc. Natl. Acad. Sci. USA **84:** 6953–6957

22 Blake C. C. F., Serpell L. C., Sunde M. and Lundgren E. (1996). A molecular model of the amyloid fibril. In: CIBA Symposium No. 199, The Nature and Origin of Amyloid Fibrils, pp. 6–21, Bock G. R. and Goode J. A. (eds), John Wiley and Sons Ltd, Chichester

23 Blake C. C. F. and Serpell L. C. (1996) Synchrotron X-ray studies suggest that the core of the transthyretin amyloid fibril is a continuous β-sheet helix. Structure **4:** 989–998

24 Blake C. C. F., Geisow M. J., Oatley S. J., Rerat B. and Rerat C. (1978). Structure of prealbumin: secondary, tertiary and quaternary interactions determined by Fourier refinement at 1.8 Å. J. Mol. Biol. **121:** 339–356

25 Richardson J. (1981) The anatomy and taxonomy of protein structure. Adv. Protein Chem. **34:** 167–339

26 Saraiva M. J. M. (1995) Transthyretin mutations in health and disease. Hum. Mutation **5:** 191–196

27 Vidal R., Garzuly F., Budka H., Lalowski M., Linke R. P., Frangione B. et al. (1996) Meningocerebrovascular amyloidosis associated with a novel transthyretin mis-sense mutation at codon-18. Am. J. Pathol. **148:** 361–366

28 Terry C. J., Damas A. M., Oliviera P., Saraiva M. J. M., Alves A. L., Costa P. P. et al. (1993) Structure of Met30 variant of transthyretin and its amyloidogenic variations. EMBO J. **12:** 735–741

29 Hamilton J., Steinrauf L., Braden B., Liepnieks J., Benson M., Holmgren G. et al. (1993) The X-ray crystal structure refinements of normal human transthyretin and the amyloidogenic Val-30-Met variant to 1.7 Å resolution. J. Biol. Chem. **268:** 2416–2424

30 Steinrauf L. K., Hamilton J. A., Braden B. C., Murrell J. R. and Benson M. D. (1993) X-ray crystal structure of the Ala109Thr variant of human transthyretin which produces euthyroid hyperthyroxinemia. J. Biol. Chem. **268:** 2425–2430

31 Saraiva M. J. M., Almeida M. R., Alves I. L., Bonifacio M. J., Damas A. M., Palha J. A. et al. (1996) Modulating conformational factors in transthyretin amyloid. In: CIBA Symposium No. 199, The Nature and Origin of Amyloid Fibrils, pp. 6–21, Bock G. R. and Goode J. A. (eds), John Wiley and Sons Ltd, Chichester

32 Thylen C., Wahlchrist J., Haetner E., Sandgren O., Holmgren G. and Lundgren E. (1993) Modifications of transthyretin in amyloid fibrils: analysis of amyloid from homozygous and heterozygous individuals with the Met30 mutation. EMBO J. **12:** 743–748

33 McCutchen S. and Kelly J. W. (1993) Intermolecular disulphide linkages are not required for transthyretin amyloid fibril formation in vitro Biochem. Biophys. Res. Commun. **197:** 415–421

34 Damas A. M., Ribeiro S., Lamzin V. S., Palha J. A. and Saraiva M. J. (1996) Structure of Val122Ile variant transthyretin – a cardiomyopathic mutant. Acta Crystallogr. D **52:** 966–972

35 Serpell L. C. and Blake C. C. F. (1994). In: Amyloid and Amyloidosis, pp. 447–450, Kisilevsky, R., Benson, M. D., Frangione, B., Gauldie, J., Muckle, T. J. and Youngs, I. D. (eds), Parthenon Publishing Group Inc., New York

36 Serpell L. C., Goldsteins G., Dacklin I., Lundgren E. and Blake C. C. F. (1996) The 'edge strand' hypothesis: prediction and test of a mutational 'hot-spot' on the transthyretin molecule associated with FAP amyloidogenesis. Amyloid: Int. J. Exp. Clin. Invest. **3:** 75–85

37 Kelly J. W. and Lansbury P. T. (1994) A chemical approach to elucidate the mechanism of transthryretin and β-protein amyloid fibril formation. Amyloid: Int. J. Exp. Clin. Invest. **1:** 186–205

38 Kelly J. W. (1996) Alternative conformations of amyloidogenic proteins govern their behaviour. Curr. Opin. Struct. Biol. **6:** 11–17

39 Rosen H. N., Moses A. C., Murrell J. R., Liepnieks J. J. and Benson M. D. (1993) Thyroxine interactions with transthyretin – a comparison of 10 different naturally occurring human transthyretin variants. J. Clin. Endocrinol. Metabol. **77:** 370–374

40 Colon W. and Kelly J. W. (1992) Partial denaturation of transthyretin is sufficient for amyloid fibril formation in vitro. Biochemistry **31:** 8654–8660

41 Pepys M. B., Hawkins P. N., Booth D. R., Vigushin D. M., Tennet G. A., Soutar A. K. et al. (1993) Human lysozyme gene mutations cause hereditary systemic amyloidosis. Nature **362:** 553–557

42 Artymiuk P. J. and Blake C. C. F. (1981) Refinement of human lysozyme at 1.5 Å resolution: analysis of non-bonded and hydrogen-bond interactions. J. Mol. Biol. **152:** 737–762

43 Redfield C. and Dobson C. M. D. (1990) ^{1}H NMR Studies of human lysozyme: spectral assignment and comparison with hen lysozyme. Biochemistry **29:** 7201–7214

44 Radford S. E., Dobson C. M. and Evans P. A. (1992) The folding of hen lysozyme involves partially structured intermediates and multiple pathways. Nature **358:** 302–307

45 Hooke S. D., Radford S. E. and Dobson C. M. (1994) The refolding of human lysozyme: a comparison with the structurally homologous hen lysozyme. Biochemistry **33:** 5867–5876

46 Booth D. R., Sunde M., Bellotti V., Robinson C. V., Hutchinson, W. L., Fraser P. E. et al. (1997) Instability, unfolding and fibrillogenesis in amyloidogenic lysozyme variants. Nature **385:** 787–793

47 Adams M. J., Blundell T. L., Dodson E. J., Dodson G. G., Vijayan M., Baker E. N. et al. (1969) The structure of rhombohedral 2 zinc insulin crystals. Nature **224:** 491–495

48 Bode W., Engh R., Musil D., Thiele U., Huber R., Karshikov A. et al. (1988) The 2.0 Å X-ray crystal structure of chicken egg white cystatin and its possible mode of interaction with cysteine proteinases. EMBO J. **7:** 2593–2599

49 Burtnick L. D., Robinson R. C. and Koepf E. K. (1996) The structure of horse plasma gelsolin to 2.5 Å. Biophys. J. **70:** Pt. 2, pSUA12

50 Riek R., Hornemann S., Wider G., Billeter M., Glockshuber R. and Wüthrich K. (1996) NMR structure of the mouse prion protein domain PrP(121–231). Nature **382:** 180–182

51 Nolte R. T. and Atkinson D. (1992) Conformational analysis of apolipoprotein A-1 and E-3 based on primary sequence and circular dichroism. Biophys. J. **63:** 1221–1239

52 Poljak R. J., Amzel L. M., Avey H. P., Chen B. L., Phizackerley R. P. and Saul F. (1973) The three-dimensional structure of a Fab fragment of a human immunoglobulin at 2.8 Å resolution. Proc. Natl. Acad. Sci. USA **70:** 3305–331

53 Becker J. and Reeke G. (1985) Three-dimensional structure of β_2-microglobulin. Proc. Natl. Acad. Sci. USA **82:** 4225–4229

54 Hilbich C., Kisters-Woike B., Reed J., Masters C. and Beyreuther K. (1991) Aggregation and secondary structure of synthetic amyloid βA4 peptides of Alzheimer's disease. J. Mol. Biol. **218:** 149–163

55 Sticht H. P., Bayer P., Willbold D., Dames S., Hilbich C., Beyreuther K. et al. (1995) Structure of amyloid A4(1-40)-peptide of Alzheimer's disease. Eur. J. Biochem. **233:** 293–298

56 Soto C., Castano E., Frangione B. and Inestrosa N. (1995) The α-helical to β-sheet transition in the amino-terminal fragment of the amyloid β-peptide modulates amyloid formation. J. Biol. Chem. **270:** 3063–3067

57 Kirshenbaum K. and Daggett V. (1995) pH-Dependent conformations of the amyloid β(1–28) peptide fragment explored using molecular dynamics. Biochemistry **34:** 7629–7639

58 Kirshenbaum K. and Daggett V. (1995) Sequence effects on the conformational properties of the amyloid β(1–28) peptide: testing a proposed mechanism for the $\alpha \rightarrow \beta$ transition. Biochemistry **34:** 7640–7647

59 Barrow C. J., Yasuda A., Kenny P. T. M. and Zagorski M. G. (1992). Solution conformations and aggregational properties of synthetic amyloid β- peptides of Alzheimer's disease. J. Mol. Biol. **225:** 1075–1093

60 Terzi E., Holzemann G. and Seelig J. (1994) Reversible random coil-β-sheet transition of the Alzheimer β-amyloid fragment (25–35). Biochemistry **33:** 1345–1350

61 Pan K.-M., Baldwin M. A., Nguyen J. T., Gaseet M., Serban A., Groth D. et al. (1993) Conversion of α-helices into β-sheets features in the formation of the scrapie prion proteins. Proc. Natl. Acad. Sci. USA **90:** 10962–10966
62 Huang Z., Gabriel J.-M., Baldwin M. A., Fletterick R. J., Prusiner S. B. and Cohen F. E. (1994) Proposed 3-dimensional structure for the cellular prion protein. Proc. Natl. Acad. Sci. USA **91:** 7139–7143
63 Gasset M., Baldwin M. A., Lloyd D. H., Gabriel J.-M., Holtzman D. M., Cohen F. E. et al. (1992) Predicted α-helical regions of the prion protein, when synthesized as peptides form amyloid. Proc. Natl. Acad. Sci. USA **89:** 10940–10944
64 Gasset M., Baldwin M., Fletterick R. and Prusiner S. (1993) Perturbation of secondary structure of the scrapie prion protein under conditions that alter infectivity. Proc. Natl. Acad. Sci. USA **90:** 1–5
65 Cohen F. E., Pan K.-M., Huang Z., Baldwin M., Fletterick R. and Prusiner, S. B. (1994) Structural clues to prion replication. Science **264:** 530–531
66 Safar J., Roller P., Gajdusek D. and Gibbs C. (1994) Scrapie amyloid (prion) has the conformational characteristics of an aggregated molten globular folding intermediate. Biochemistry **33:** 8375–8383
67 McCutchen S., Colon W. and Kelly J. W. (1993) Transthyretin mutation Leu-55-Pro significantly alters tetramer stability and increases amyloidogenicity. Biochemistry **32:** 12119–12127
68 McCutchen S. L., Lai Z., Miroy G. J., Kelly J. W. and Colon W. (1995) Comparison of lethal and nonlethal transthyretin variants and their relationship to amyloid disease. Biochemistry **34:** 13527–13536
69 Prusiner S. B. (1996) Molecular biology and pathogenesis of prion diseases. Trends Biochem. Sci. **21:** 482–487
70 Caughey B. and Chesebro B. (1997) Prion protein and the transmissible spongiform encephalopathies. Trends Cell Biol. **7:** 56–62
71 Harrison P. M., Bamborough P., Daggett V., Prusiner S. B. and Cohen F. E. (1997) The prion folding problem. Curr. Opin. Struct. Biol. **7:** 53–59
72 Telling G. C., Parchi P., DeArmond S. J., Cortelli P., Montagna P., Gabizon R. et al. (1996) Evidence for the conformation of the pathological isoform of the prion protein enciphering and propagating prion diversity. Science **274:** 2079–2082
73 Kraulis, P. J. (1991) Molscript: a program to produce both detailed and schematic plots of protein structures. J. Appl. Crystallogr. **24:** 946–950